

A 3D Search for the Interplay between AGN and Star Formation in Galaxies

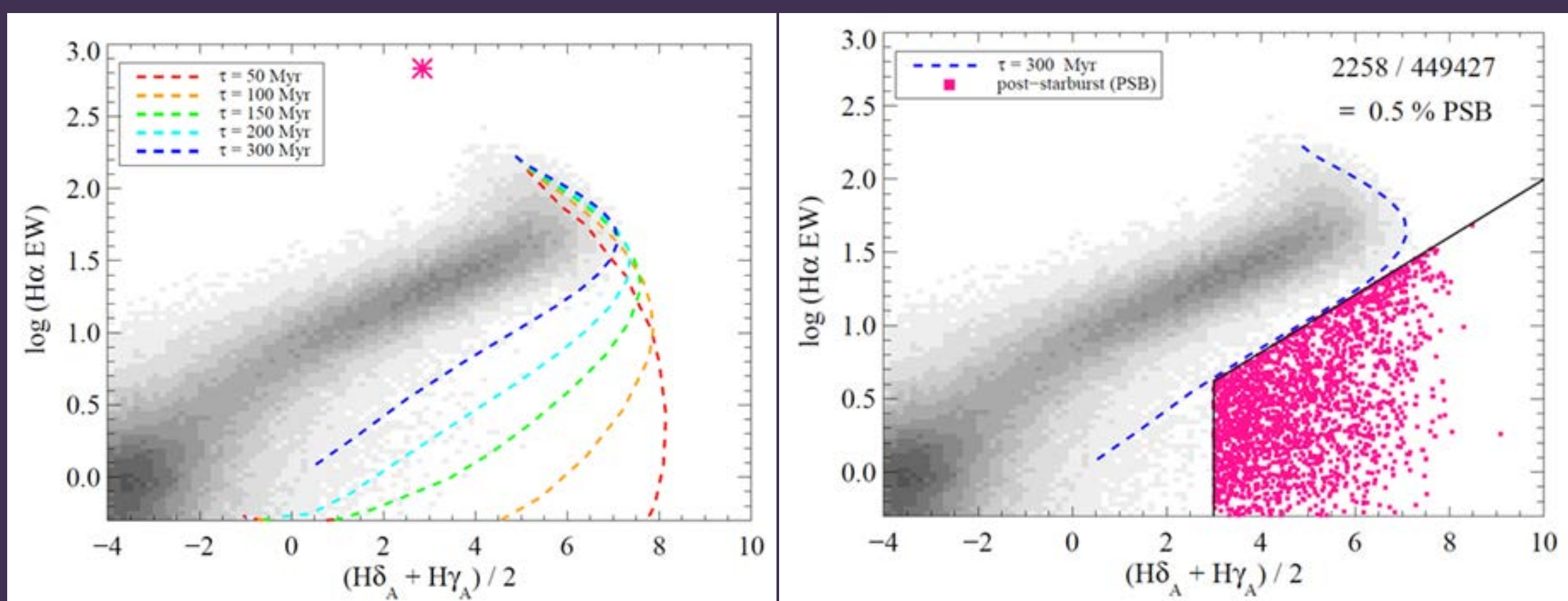
Marsha Wolf,¹ Eric Hooper,¹ Ryan Sanders,² Charles Liu³

¹University of Wisconsin – Madison, ²UCLA, ³CUNY – Staten Island

ABSTRACT

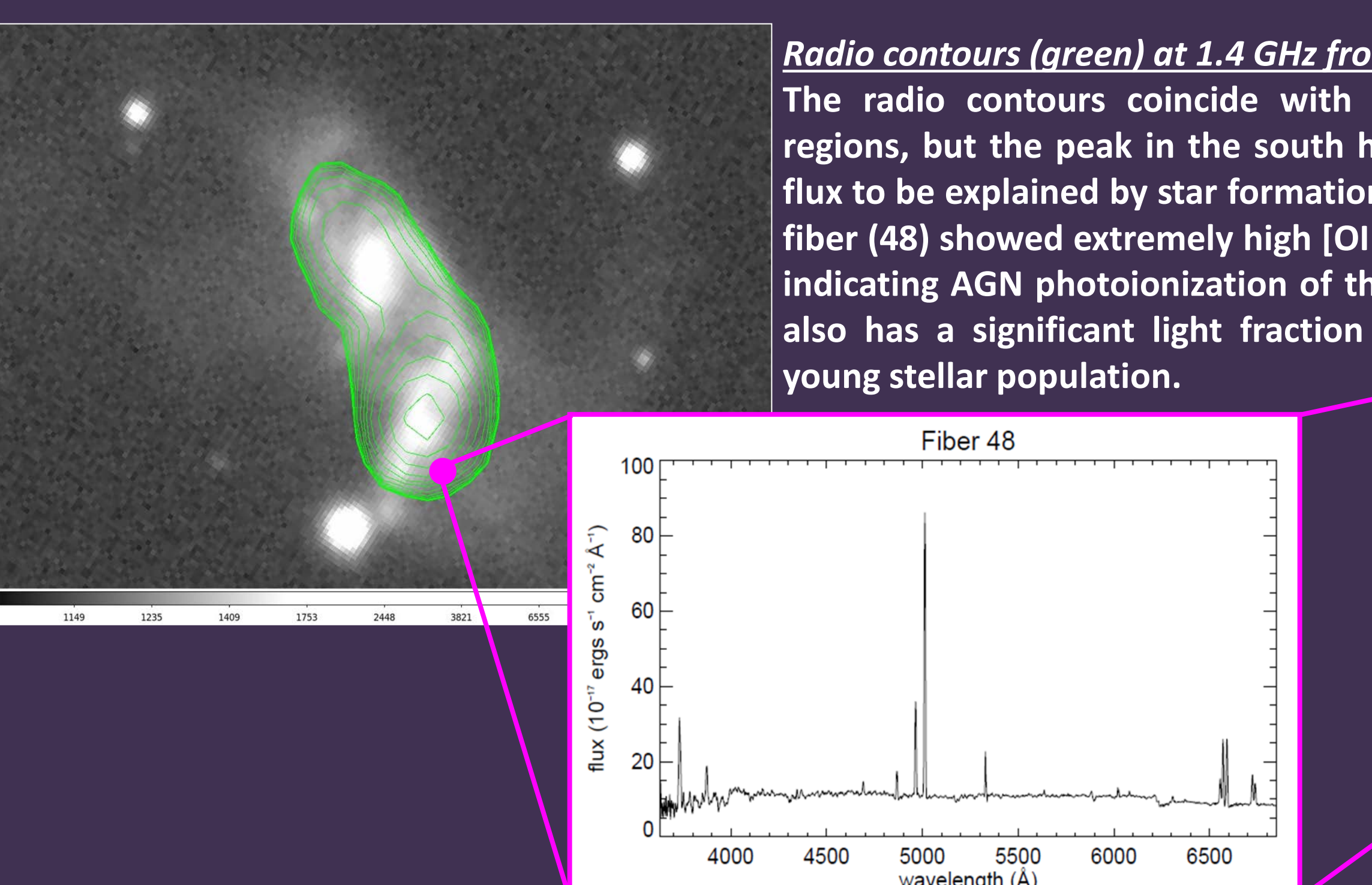
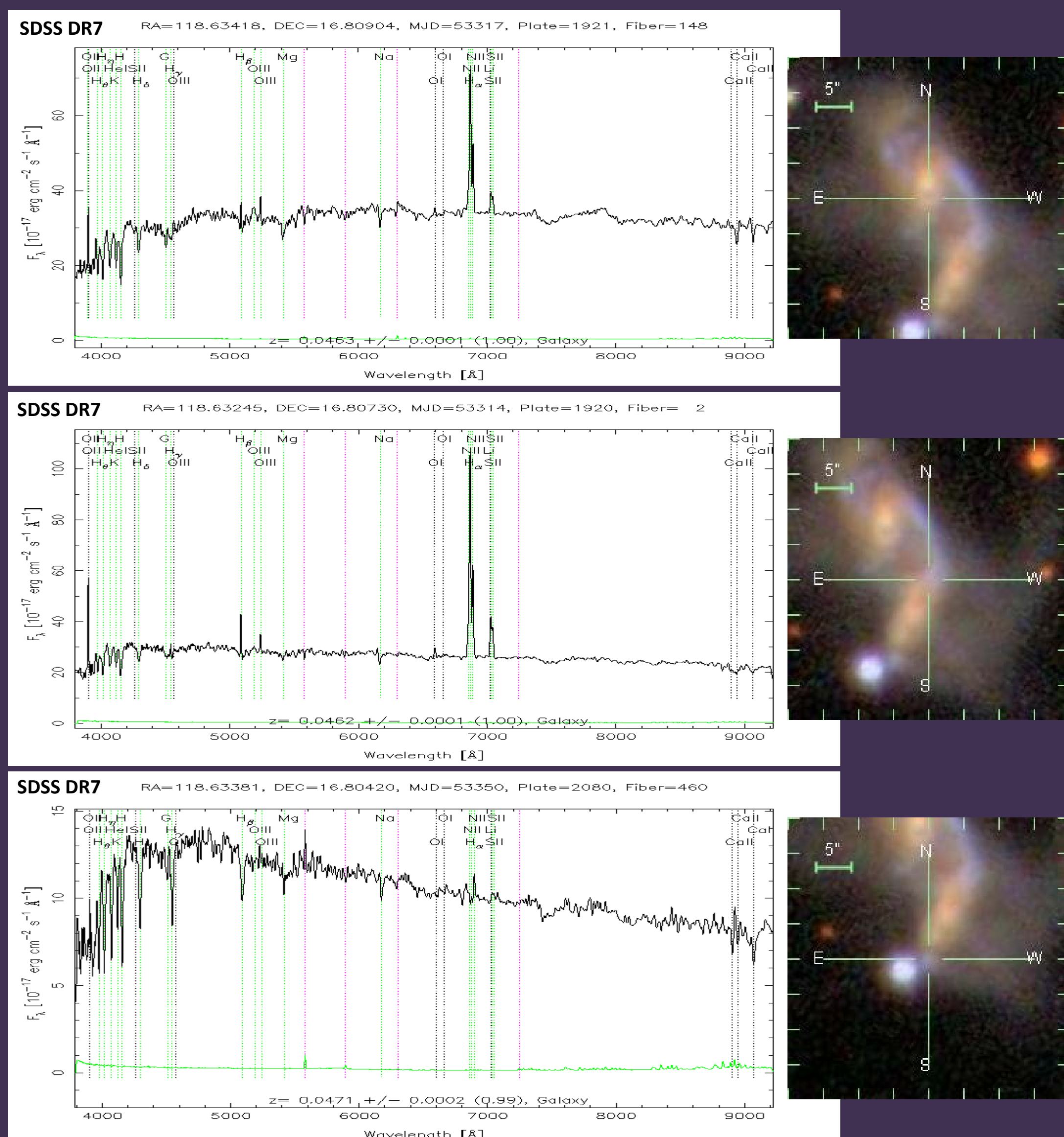
Integral field optical spectroscopy, near infrared imaging, and radio interferometry are a very powerful combination of tools for studying the interplay between AGN and star formation in galaxies. We introduce a sample of SDSS galaxies with selection criteria designed to maximize our chances of catching both processes in action. The galaxies are post-starburst, are allowed, but not required, to have ongoing star formation, and potentially contain radio AGN. The resulting sample includes not only objects classified as traditional post-starbursts, but also ones that would have been classified as Seyferts based on their emission line properties alone. The systems span a range of merger phases from initial interaction to fully merged, providing snapshots throughout the entire sequence. We are compiling a multi-wavelength data set, including spatially resolved optical spectra using IFUs on WIYN, near infrared images using WHIRC on WIYN, and continuum radio maps from the VLA and GMRT. Here we present initial results highlighting the power of 3D observations. A prime example is J0754+1648, an interacting system in which we see a post-starburst region near a radio AGN surrounded by highly ionized gas. We will be investigating possible signs of an outflow in this region with a new higher spatial resolution IFU, which may confirm a scenario of star formation truncation by AGN feedback. The galaxy system shows a large amount of ongoing star formation in regions farther removed from the AGN. Overall, the system appears to be transitioning between the starburst/AGN and post-starburst phase.

SAMPLE SELECTION



Tremonti's selection of post-starburst galaxies from SDSS DR7. **LEFT:** The locus of DR7 galaxies in $H\alpha$ equivalent width and an average of the $H\delta_A$ and $H\gamma_A$ Lick indices. The evolution of Bruzual & Charlot (2003) stellar population synthesis models for different starburst e-folding times, τ , are overplotted as dashed lines. **RIGHT:** The $\tau = 300$ Myr line was chosen to trace the edge of the main locus of galaxies in the strong Balmer absorption line – low $H\alpha$ emission line post-starburst galaxy regime. A total of 2816 (magenta squares) out of 449,427 galaxies fall into this category (0.6%).

J0754+1648: A SYSTEM IN TRANSITION



Radio contours (green) at 1.4 GHz from FIRST. The radio contours coincide with star forming regions, but the peak in the south has too much flux to be explained by star formation alone. One fiber (48) showed extremely high $[OIII]\lambda 5007$ flux, indicating AGN photoionization of the oxygen. It also has a significant light fraction from a very young stellar population.

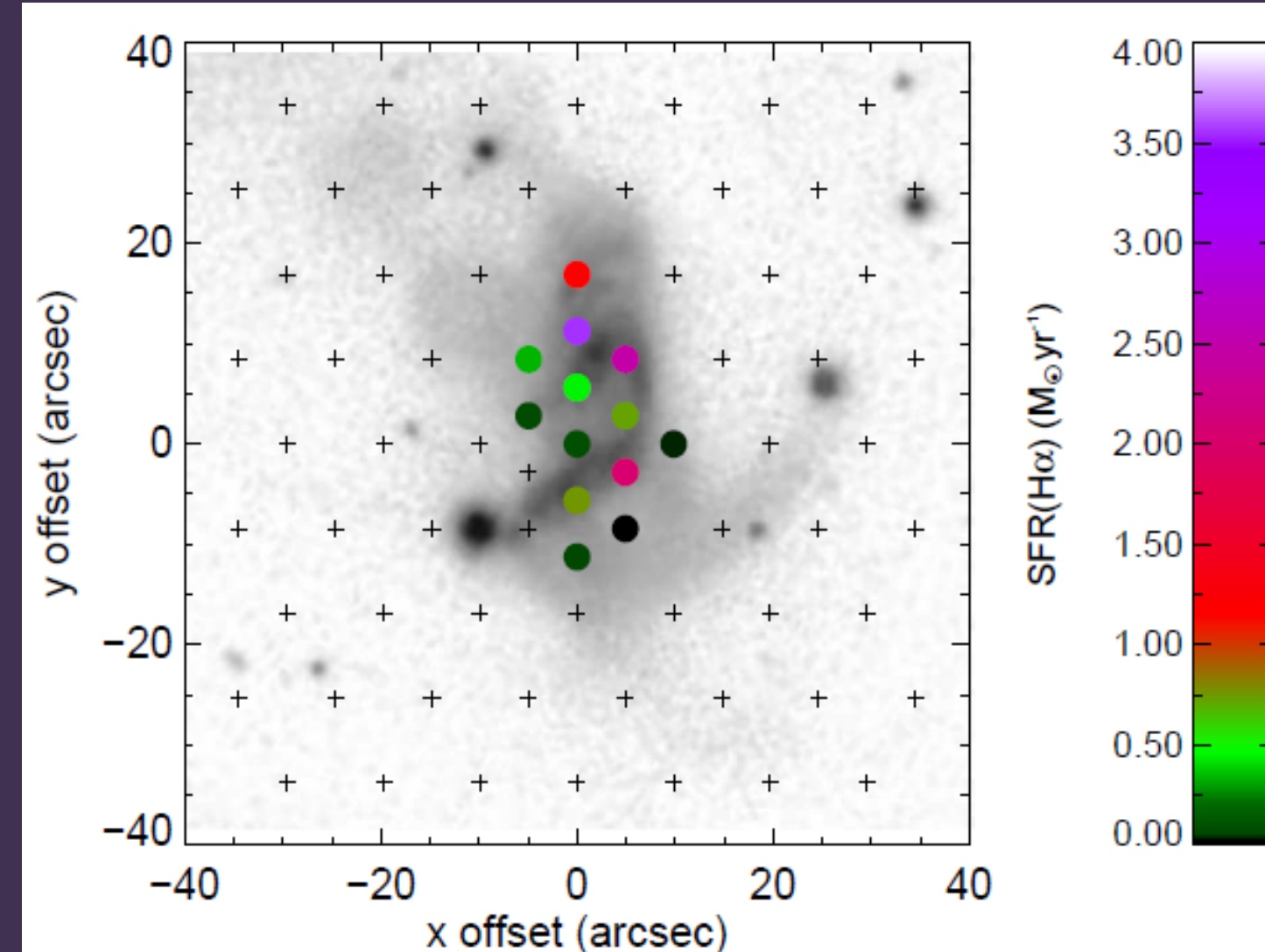
OBSERVATIONS & ANALYSIS

We obtained spectra on the WIYN 3.5-meter telescope at KPNO using the SparsePak IFU, which feeds a bench spectrograph. SparsePak features 82 fibers, each 5" in diameter, packed in a dense core surrounded by a more sparsely populated field of fibers. We collected 5 hours of integration on the object across the entire optical band using the fiber orientation pictured below. The data were reduced in IRAF using the hydra package.

We use IDL code by Tremonti to fit simple stellar populations to the continuum and measure emission line fluxes. We use Osterbrock (1989) to make reddening corrections and the Kennicutt (1998) $H\alpha$ calibration to estimate star formation rates using a standard cosmology. We fit the continuum with simple stellar populations drawn from the Bruzual and Charlot (2003) models, using 10 ages ranging from 5 Myr to 10 Gyr and 6 metallicities ranging from $Z=0.0001$ to $Z=0.05$. Since we only have spectra in optical wavelengths, there is a significant age/metallicity degeneracy when fitting model spectra. Rather than determining both age and metallicity from stellar pop models, we use the R_{23} ratio and calibration by Zaritsky et al. (1994) to find the oxygen abundance in each fiber and, with the assumption that the stellar population has solar oxygen abundance, calculate the $[Fe/H]$ from it. Models of that metallicity are then fit to the spectrum of each fiber to determine the stellar population ages.

STAR FORMATION RATES

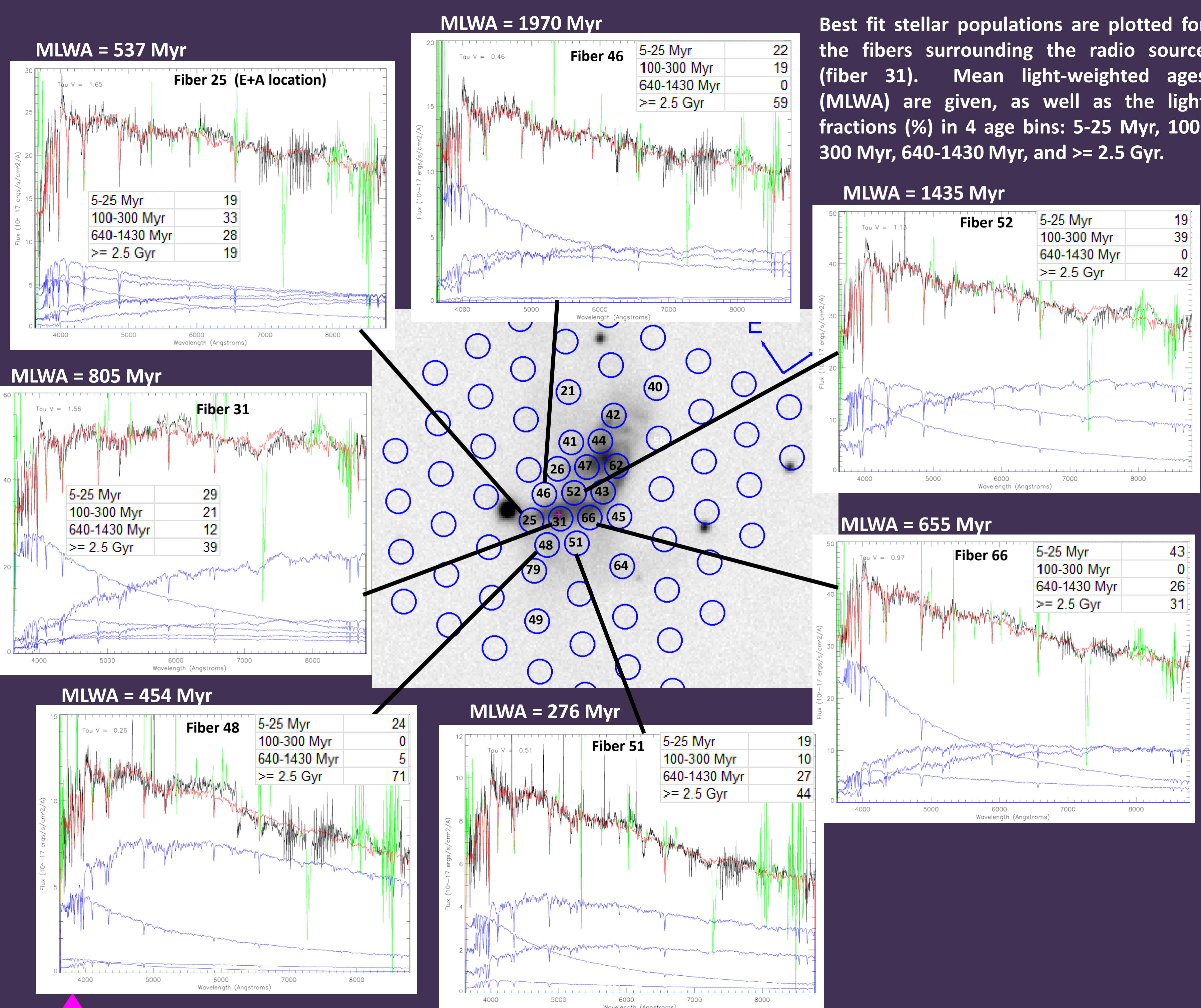
Star Formation Rate (SFR) estimates.



Heavier star formation is more prominent toward the upper region, well removed from the post-starburst signature, which is concentrated more toward the lower regions.

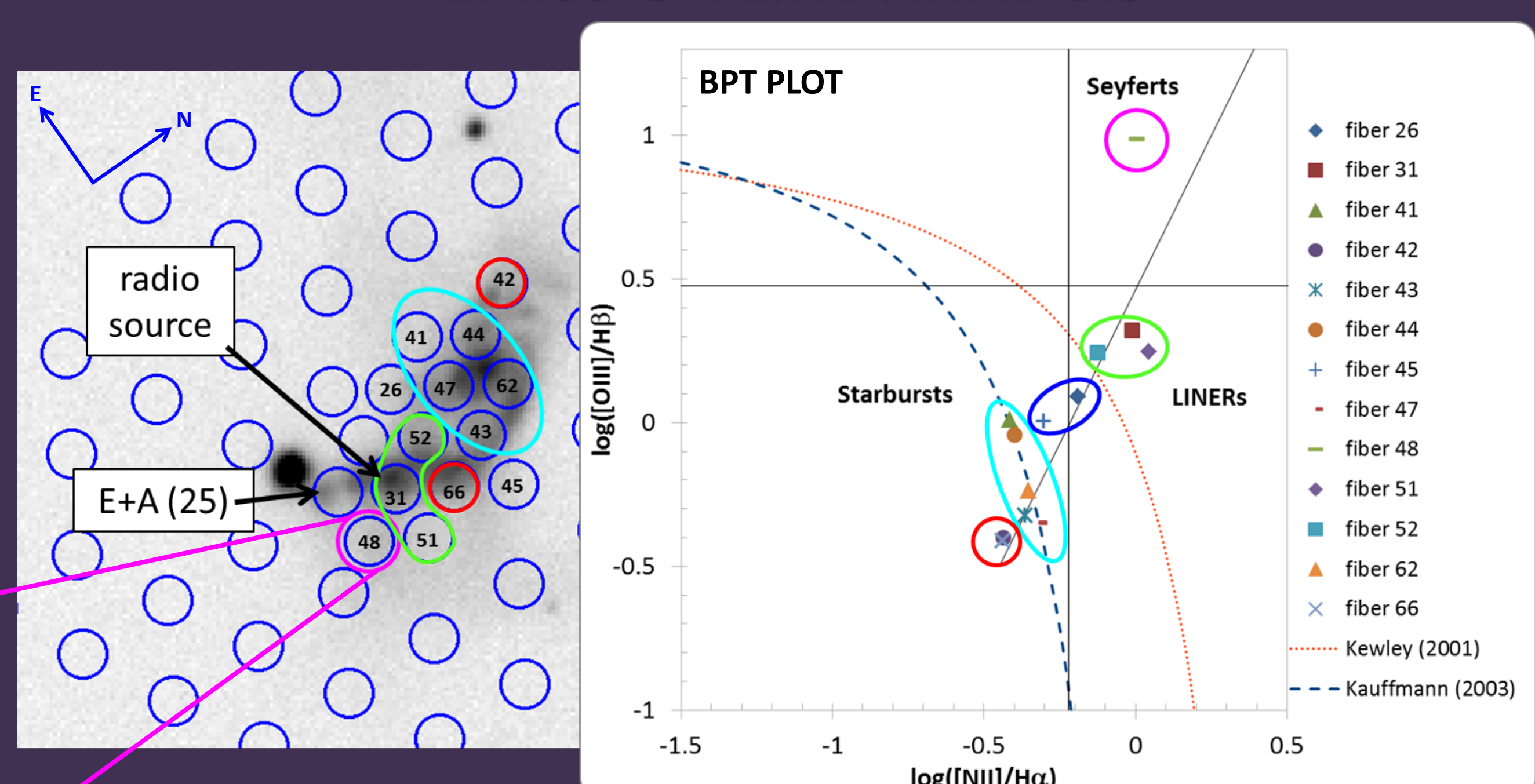
The highest rate in an individual fiber is $3.5 M_{\odot} \text{yr}^{-1}$. Summing the star formation rates in individual fibers yields a lower limit for the total system star formation rate of $>11.6 M_{\odot} \text{yr}^{-1}$.

STELLAR POPULATIONS



Best fit stellar populations are plotted for the fibers surrounding the radio source (fiber 31). Mean light-weighted ages (MLWA) are given, as well as the light fractions (%) in 4 age bins: 5-25 Myr, 100-300 Myr, 640-1430 Myr, and ≥ 2.5 Gyr.

EMISSION LINE ANALYSIS



5-25 Myr	24
100-300 Myr	0
640-1434 Myr	5
≥ 2.5 Gyr	71
5-25 Myr	22 ± 6
100-300 Myr	23 ± 15
640-1434 Myr	13 ± 13
≥ 2.5 Gyr	42 ± 3
5-25 Myr	18 ± 2
100-300 Myr	19 ± 20
640-1434 Myr	13 ± 9
≥ 2.5 Gyr	35 ± 22
5-25 Myr	47 ± 7
100-300 Myr	6 ± 11
640-1434 Myr	4 ± 9
≥ 2.5 Gyr	43 ± 7
5-25 Myr	50 ± 10
100-300 Myr	0 ± 0
640-1434 Myr	13 ± 18
≥ 2.5 Gyr	37 ± 8

FUTURE WORK:

- Observe with new HexPak IFU on WIYN for higher spatial resolution around the AGN and post-starburst regions. Look for signs of outflow from the AGN.
- Refine the model basis set for stellar population modeling – decrease the number of models in a statistically robust way using diffusion k-means (e.g. Mosby+ in prep).